

2mic

PSU-IRL-SCI-421 E

Classification Numbers 3.2.2



THE PENNSYLVANIA
STATE UNIVERSITY

IONOSPHERIC RESEARCH

Scientific Report 421 E

ULTRAVIOLET SOURCE FOR ROCKET MEASUREMENTS OF NITRIC OXIDE IN THE UPPER ATMOSPHERE

by

Javed M. H. Siddiqui

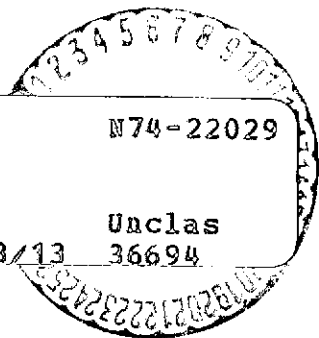
March 1, 1974

*The research reported in this document has been supported
by the U.S. Army Research Office under Contract Grant No.
DA-ARO-D-31-124-72-G158 and the National Aeronautics and
Space Administration under Contract Grant No. NGR 39-009-
218.*

IONOSPHERE RESEARCH LABORATORY



(NASA-CR-136909)	ULTRAVIOLET SOURCE FOR	N74-22029
ROCKET MEASUREMENTS OF NITRIC OXIDE IN		
THE UPPER ATMOSPHERE (Pennsylvania State		
Univ.)	55 p HC \$5.75	CSCI 04A
		Unclas
		G3/13 36694



University Park, Pennsylvania

DOCUMENT CONTROL DATA - R & D

(Security classification of title, body of abstract and indexing annotation must be entered when the overall report is classified)

1. ORIGINATING ACTIVITY (Corporate author)		2a. REPORT SECURITY CLASSIFICATION	
The Ionosphere Research Laboratory			
		2b. GROUP	
3. REPORT TITLE			
Ultraviolet Source for Rocket Measurements of Nitric Oxide in the Upper Atmosphere			
4. DESCRIPTIVE NOTES (Type of report and, inclusive dates)			
Scientific Report			
5. AUTHOR(S) (First name, middle initial, last name)			
Javed M. H. Siddiqui			
6. REPORT DATE		7a. TOTAL NO. OF PAGES	7b. NO. OF REFS
March 1, 1974		53	
8a. CONTRACT OR GRANT NO.		9a. ORIGINATOR'S REPORT NUMBER(S)	
DA-ARO-D-31-124-72-G158		PSU-IRL-SCI-421 E	
b. PROJECT NO.		9b. OTHER REPORT NO(S) (Any other numbers that may be assigned this report)	
NGR 39-009-218			
c.			
d.			
10. DISTRIBUTION STATEMENT			
Supporting Agencies			
11. SUPPLEMENTARY NOTES		12. SPONSORING MILITARY ACTIVITY	
		U. S. Army Research Office National Aeronautics and Space Administration	
13. ABSTRACT			
<p>An ultraviolet source suitable for balloon and rocket payloads for measurements of nitric oxide in the lower D-region of the ionosphere has been developed. The source primarily emits 1236 Å and 1165 Å photons obtained from an r. f. -excited krypton discharge in a resonator of coaxial geometry. Ultraviolet flux output greater than 10^{14} photons/sec can be obtained from this source.</p> <p>A systematic design philosophy is developed which enables the photon output to be optimized with respect to photon wavelength, gas pressure, r. f. frequency, resonator geometry, and gas to be used. Critical factors in the design are discussed in detail.</p>			

PSU-IRL-SCI-421 E
Classification Number 3.2.2

Scientific Report 421 E

Ultraviolet Source for Rocket
Measurements of Nitric Oxide in the Upper Atmosphere

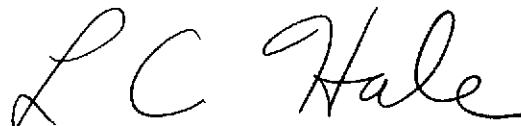
by

Javed M. H. Siddiqui

March 1, 1974

The research reported in this document has been supported by the U. S. Army Research Office under Contract Grant No. DA-ARO-D-31-124-72-G158 and the National Aeronautics and Space Administration under Contract Grant No. NGR 39-009-218.

Submitted by:



L. C. Hale, Professor of
Electrical Engineering
Project Supervisor

Approved by:



J. S. Nisbet, Director
Ionosphere Research Laboratory

Ionosphere Research Laboratory
The Pennsylvania State University
University Park, Pennsylvania 16802

ia

ACKNOWLEDGEMENTS

I wish to thank Dr. L. C. Hale and Dr. D. R. Voltmer for their invaluable guidance and encouragement.

This research was supported by the U.S. Army Research Office, Durham, North Carolina, Grant DA-ARO-D-31-124-72-G158 and by the National Aeronautics and Space Administration Grant NGR 39-009-218.

TABLE OF CONTENTS

	Page
ACKNOWLEDGEMENTS	ii
LIST OF FIGURES	v
ABSTRACT	vi
I INTRODUCTION	1
1.1 General Statement of the Problem	1
II THEORETICAL BACKGROUND	3
2.1 Photon Production and Choice of Discharge Gas	3
2.2 Emission of Radiation	6
2.3 Energy Transferral Phenomena	6
2.3.1 Infrequency Electron-Molecular Collisions ($\nu \ll f$)	7
2.3.2 Electron-Molecular Collision nearly once each r. f. Cycle ($f_1 \lesssim \nu \lesssim f_2$, where $f_1 = \nu/10$ and $f_2 = 10\nu$)	8
2.3.3 Frequent Electron-Molecular Collisions ($\nu \gg f$)	12
2.4 Selection of Optimal r. f. Frequency and Pressure (Collision Frequency)	12
III DESIGN OF THE ULTRAVIOLET SOURCE	14
3.1 Background	14
3.2 Design of the Lower Frequency Source	14
3.3 Design of the Higher Frequency Source (900 MHz $\lesssim \nu \lesssim$ 9000 MHz)	23
IV RESULTS AND INTERPRETATIONS	28
4.1 Optimum Photon Output as a Function of Gas, Pressure and Frequency, etc.	28

	Page
4.2 Saturation of Photon Output with Increased Input Power	29
4.3 Effect of Superimposing DC Field on AC Field	30
4.4 Ionization Field	31
V CONCLUSIONS	32
APPENDIX A	33
APPENDIX B	39
REFERENCES	46

LIST OF FIGURES

Figure	Page
2.1 Radiation Processes in Gases	4
3.1 Ratio of Electron Collision Frequency to Pressure for Hydrogen and Krypton as a Function of Frequency .	15
3.2 Schematic for Lower Frequency Source	17
3.3 Experimental Breakdown Data in Hydrogen	21
3.4 Family of Curves for a vs. p for Minimum Breakdown Field	22
3.5 High Frequency Breakdown Voltage Between Coaxial Cylinders as a Function of b/a and pa	24
3.6 Schematic of the "Stepped" Cavity Version of the Higher Frequency Source	26
A.1 Gas Container for the Lower Frequency Source	35
B.1 High Frequency Ionization Coefficient as a Function of E/p and $p\lambda$	41
B.2 Slope of ζ versus E/p Curve on Log Plot from Figure B.1	43
B.3 Solution of Equation (B.8)	45

ABSTRACT

An ultraviolet source suitable for balloon and rocket payloads for measurements of nitric oxide in the lower D-region of the ionosphere has been developed. The source primarily emits 1236 Å and 1165 Å photons obtained from an r. f. -excited krypton discharge in a resonator of coaxial geometry. Ultraviolet flux output greater than 10^{14} photons/sec can be obtained from this source.

A systematic design philosophy is developed which enables the photon output to be optimized with respect to photon wavelength, gas pressure, r. f. frequency, resonator geometry, and gas to be used. Critical factors in the design are discussed in detail.

CHAPTER I

INTRODUCTION

1.1 General Statement of the Problem

In 1963 R. A. Young (Whitten and Poppoff, 1965) suggested a technique for measuring nitric oxide in the lower D-region of the ionosphere. This technique consists of sending a suitable source of radiation (one which would photo-ionize only the nitric oxide) into the lower D-region and measure the ionization caused by the source.

For the measurement of nitric oxide by the Young technique a compact, rugged, and lightweight ultraviolet source with sufficiently high photon output (which must radiate above 1119 \AA , but below 1340 \AA , so as to ionize nitric oxide only) was required. Several types of vacuum ultraviolet sources have been developed and have been described extensively in the literature; all have been constructed basically along the same lines. Generally, they consist of a container filled with a suitable gas under low pressure fitted at one end with a window that will transmit the photon wavelengths desired. At very high frequencies the container is a resonant cavity in which the discharge is maintained by coupling energy from a microwave generator. At lower frequencies the container is typically a capacitive portion of a resonant circuit in which the discharge is maintained at resonance.

A compact Lyman- α (1216 \AA) source was built by Gee (1966). The source consisted of a quarter wave coaxial cavity shorted at one end and fitted with a lithium flouride window at the open end. R. f. energy was coupled into the cavity by a loop at the shorted end from

a 1680 MHz 1/2 watt r.f. output R. C. A. 5794 telemetry tube. A discharge was maintained behind a lithium fluoride window with the cavity filled with hydrogen at a pressure of about 1 mm Hg. In 1970, Pontano, with slight modifications of the Gee lamp, built a source which he used in his rocket borne experiment for the measurement of nitric oxide in the lower D-region of the ionosphere.

Unfortunately, the type of sources described above could not satisfy simultaneously the requirements of compactness, ruggedness, and high photon output. Thus, work was undertaken to develop a source which would meet the above requirements. In the following chapters theoretical and physical reasons which lead to an optimum design are considered.

CHAPTER II

THEORETICAL BACKGROUND

2.1 Photon Production and Choice of Discharge Gas

The molecules of a gas can exist in a number of discrete states. The ionization of the gas, i. e. , a passage of electrons through the gas, on the application of an electric field, results in exciting the molecules to various of these states. In making transitions from one state to another, the atoms emit radiation of a definite wavelength. The probability of these various transitions depends upon the nature of the gas, its pressure, etc. The processes which take place are shown in Figure 2.1. Thus, ionization is a way of producing radiation.

Wilkinson (1955) was the first to investigate the spectrum of ionized krypton. Later, Okabe (1964) investigated the resonance line of many rare gases and combination of gases under low pressure when excited by a microwave discharge; Table 1 gives the result of his work. He found that in the case of krypton the 1165 \AA line was about 23% as intense as the 1236 \AA line and that for Xe, the 1295 \AA line was about 20% of the intensity of the 1470 \AA line. On the basis of Table 1 and these considerations, it appears that the best gas to use would be Kr or the H_2 and Ar mixture since wavelengths in the region $1118 \text{ \AA} - 1340 \text{ \AA}$ are required with a minimum of input power. The 1236 \AA is resonance radiation of Kr, i. e. , it is the result of a transition of a Kr atom from the lowest excited state to the normal state. In particular, according to Wilkinson (1955), the resonance radiation of Kr results from a $^3\text{P}_1 - ^1\text{S}_0$ transition.

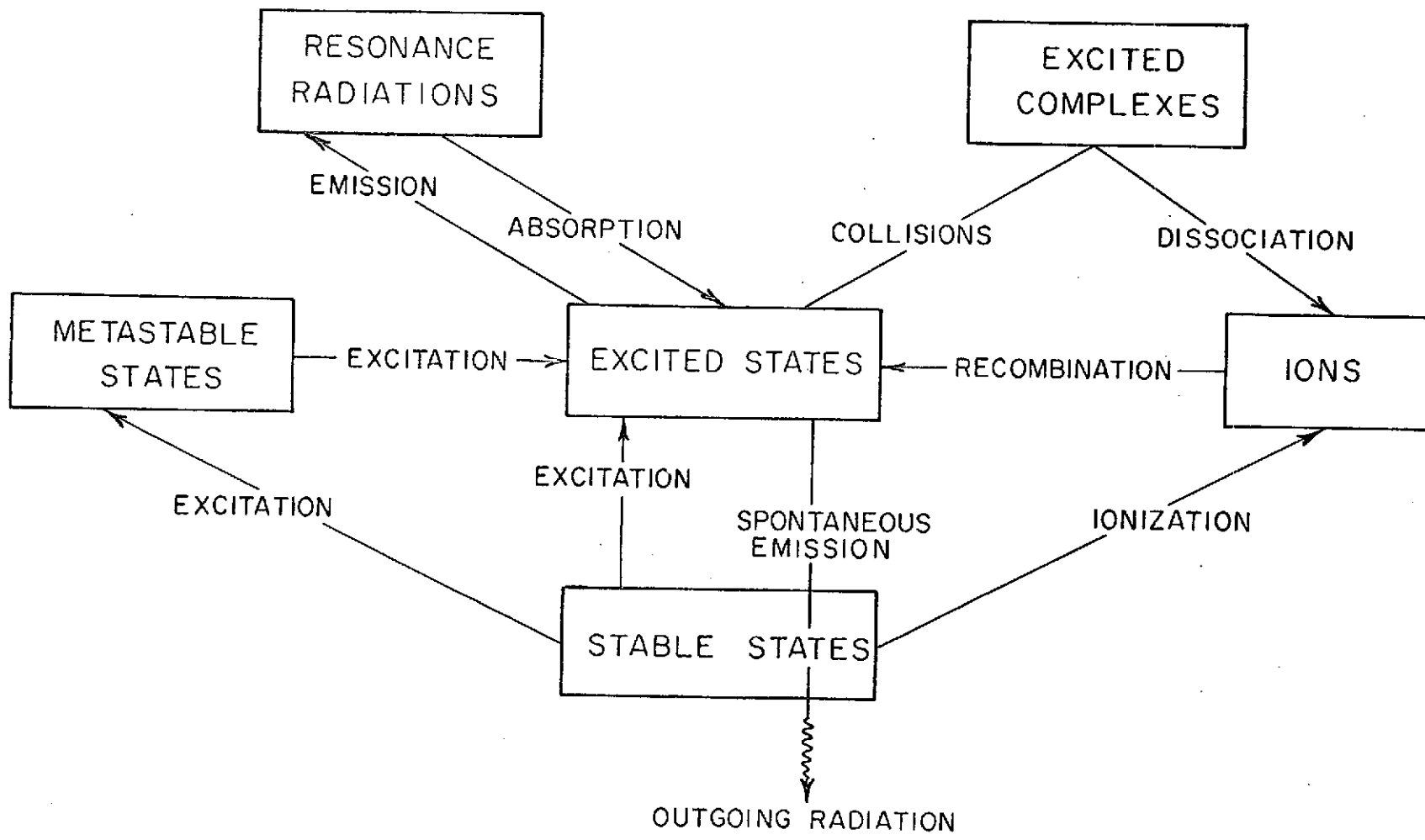


Figure 2.1 Radiation Processes in Gases

Table 1 (From Okabe)

	Pressure m.m. Hg.	Wavelength of Resonant Line \AA	Generator Output Watts	Yield Quanta/Sec
Kr	1	1236, 1165	10	5.5×10^{14}
10% Kr & He	1	1236, 1165	60	1.0×10^{15}
20% Kr & He	1	1236, 1165	50	$.9 \times 10^{15}$
Xe	0.7	1470, 1295	8	6.0×10^{14}
10% Xe & He	1	1470, 1295	30	2.0×10^{15}
20% Xe & Ar	1	1470, 1295	20	1.4×10^{15}
10% H ₂ & Ar	1	1216	60	3.0×10^{14}
20% N ₂ & Ar	1	1743, -45	50	21.0×10^{14}
5% O ₂ & Ar	1	1302, -06	30	23.0×10^{13}

2.2 Emission of Radiation

The probability of resonance radiation being reabsorbed by another atom with which it collides is very high. This atom in turn may reemit the radiation, and in this way the radiation may be passed from atom to atom before it finally escapes from the discharge. If the gas pressure is high, the mean free path of the radiation will be small and the radiation will undergo many such transitions. During this process there is a strong probability that some of the atoms while in the excited resonance state may collide with an electron which has sufficient energy to cause ionization or excitation to a higher state. In either case, the radiation emitted as the atom returns to its normal state will be of a frequency other than the resonance frequency. Thus the resonance radiation which is emitted from the ionized volume are those that are at the outer layer of the discharge. The higher the pressure, the lower is the probability of the resonance radiation from within the discharge of reaching this outer layer without making a collision which results in its transformation. On the other hand, at extremely low pressures the number of atoms available to be raised into the excited state becomes very small. Thus, an optimum pressure between these two extremes exists at which the radiation escaping from the ionized volume is maximized.

2.3 Energy Transferral Phenomena

When an electric field is applied to a gas in a container quite different processes occur depending upon the frequencies of electron-gas molecule collisions (collision frequency, ν) and of the applied field, f . For convenience, three distinct situations will be

discussed individually. There are always a small quantity of free electrons present in the gas due to cosmic or atmospheric radiations. Furthermore, the container of the gas is assumed to be so large that interactions with the walls will not be significant.

2.3.1 Infrequent Electron-Molecule Collisions ($\nu \ll f$)

These conditions exist whenever the gas pressure is very low or the frequency is very high. The equation of motion of an electron starting at a point $x = 0$ with an initial velocity component, v_0 , in the direction of a uniform electric field, E , is

$$m \frac{d^2 x}{dt^2} = eE_0 \sin(\omega t + \phi) \quad (2.1)$$

where ϕ is the phase angle of the field at the instant, $t = 0$. Integrating and applying the boundary condition $dx/dt = v_0$ when $t = 0$ gives the velocity at time t ,

$$v = v_0 + \frac{eE_0}{m\omega} \left[\cos \phi - \cos(\omega t + \phi) \right] \quad (2.2)$$

and the displacement x in the direction of the field

$$x = \left[v_0 + \frac{eE_0}{m\omega} \cos \phi \right] t + \frac{eE_0}{m\omega^2} \left[\sin \phi - \sin(\omega t + \phi) \right] \quad (2.3)$$

Equation (2.3) indicates that there is a drift motion at uniform speed in the direction of the original velocity, superimposed upon which is a sinusoidal oscillation of amplitude $eE_0/m\omega^2$ which is proportional to E_0/f^2 . The electrons which are stationary when the phase of the field is zero will oscillate about their mean position. Any initial motion perpendicular to the field is unaltered.

The oscillatory component of the velocity of the electron will not absorb any energy from the field, since it is always 90 degrees out of phase with the field. If the electron moves without hitting any gas molecules, the steady component will absorb energy from and return it to the field in alternate half cycles. Hence, if the collisions are rare, very little energy is absorbed by the electrons. When these conditions exist, ionization of the gas is very improbable since the electrons rarely gain the energy required for the ionization of the gas atoms. Even low level radiation may not be possible because the electrons may never gain the energy required for excitation of the gas atoms to even lowest states.

2.3.2 Electron-Molecular Collision nearly once each
r. f. Cycle ($f_1 \lesssim \nu \lesssim f_2$, where $f_1 = \nu/10$ and
 $f_2 = 10 \nu$)

Consider only elastic collisions in which each electron loses a very small fraction ($\sim \frac{2m}{M}$) of the kinetic energy it has before colliding with the gas molecules. In doing so the energy of the electron which it had gained from the field has been nearly conserved, while the phase of its motion has been changed enabling the electron to make still further gains from the field. By this process the energy of electrons can increase until their energy is enough to excite or ionize gas molecules, the electrons gain energy from the field, and lose it in collisions to the gas molecules.

The equation of motion in the direction of the electric field of a representative electron can be written by defining a frictional force, g_v drift which is proportional to the drift velocity,

$$m \frac{dv_{\text{drift}}}{dt} = eE_0 \sin \omega t - g_{\text{v drift}} \quad (2.4)$$

A slow drift in the direction of the applied field is superimposed on the random motion of the free electrons in the gas. By assuming that the energy lost by collision is equal to the kinetic field energy gained, the average drift velocity can be obtained to a first approximation (Francis, 1960) by the calculation of the momentum gained by an electron along a collision free path, in the field direction

$$v_{\text{drift}} = C e \lambda_e E / m v_r \quad (2.5)$$

where, v_r , is the random velocity of the electrons, C is a constant close to unity which depends upon the energy distribution of the electrons, and λ_e is the average distance travelled between collisions. Rewriting Equation (2.5)

$$\frac{m}{\tau} v_{\text{drift}} = eE \quad (2.6)$$

where, τ is the average time of free flight of the electron between collisions with gas molecules, $1/\tau = \nu$. In the steady state the rate of gain of momentum by the electron is equal to the rate of loss of momentum by collision. The right-hand side of Equation (2.6) represents the rate of gain in momentum by the electron. Hence, in steady state the rate of loss in momentum is given by the left-hand side of Equation (2.6). From Equation (2.4) $eE_0 \sin \omega t = g_{\text{v drift}}$ which gives $g = \frac{m}{\tau}$. This value of g is only valid when the dimensions of the container are much greater than λ_e , and, at any instant, the

electrons are in a state of equilibrium with the field so that the terms on the right-hand side of Equation (2.4) are each much greater than the left-hand side.

Integration of Equation (2.4) gives the drift velocity of the electrons.

$$v_{\text{drift}} = \frac{dx}{dt} = \frac{eE_0}{m} \frac{\sin(\omega t - \gamma)}{\sqrt{\nu^2 + \omega^2}} \quad (2.7)$$

where

$$\tan \gamma = \frac{\omega}{\nu} \quad (2.8)$$

Further integration gives the displacement, x

$$x = \frac{eE_0}{m\omega} \frac{\cos(\omega t - \gamma)}{\sqrt{\nu^2 + \omega^2}} + \text{constant} \quad (2.9)$$

In this case it is seen that the displacement is entirely oscillatory about a mean position with an amplitude of $eE_0/m\omega \sqrt{\nu^2 + \omega^2}$. The high frequency electron current density j_e (due to the drift of n electron/cm³) is

$$j_e = nev_{\text{drift}} = \frac{ne^2E_0}{m} \frac{\sin(\omega t - \gamma)}{\sqrt{\nu^2 + \omega^2}} \quad (2.10)$$

The current lags behind the applied field by the phase angle γ . The instantaneous rate at which the electrons in unit volume gain energy is given by the instantaneous power, P , supplied by the field per unit volume, i. e., by the product VI . V , the potential across unit cube is numerically equal to the field, E , while I , the current through the unit cube is by definition j_e . Hence

$$P = E j_e = (E_o \sin \omega t) \left[\frac{ne^2}{m} E_o \frac{\sin(\omega t - \gamma)}{\sqrt{\nu^2 + \omega^2}} \right] \quad (2.11)$$

$$\frac{ne^2 E_o^2}{2m} \left[\frac{\cos \gamma - \cos 2\omega t}{\sqrt{\nu^2 + \omega^2}} \right] \quad (2.12)$$

The steady rate at which electrons gain energy and deliver it to a unit volume of the gas is given by the time average of this expression. Since $\langle \cos 2\omega t \rangle$ is zero, and using Equation (2.8)

$$P = \frac{ne^2 E_o^2}{2m} \frac{\nu}{\nu^2 + \omega^2} \quad (2.13)$$

Comparing Equation (2.13) with the steady drift motion of electrons in a DC field, where

$$P_{DC} = E_{DC} j_e = E_{DC} ne \left(\frac{e}{m} \tau E_{DC} \right) = \frac{ne^2 E_{DC}}{m\nu} \quad (2.14)$$

it is possible to define an effective steady (DC) field E_{eff} which would transfer energy to electrons at the same rate as the actual applied high frequency field whose root mean square value is E_{rms} ($= E_o / \sqrt{2}$). From Equations (2.13) and (2.14) the relationship is

$$E_{eff}^2 = E_{rms}^2 \frac{\nu^2}{\nu^2 + \omega^2} \quad (2.15)$$

Hence it is seen that the effectiveness of the electric field in transferring energy to the electrons is modified by the quantity $\nu^2 / \nu^2 + \omega^2$. Equation (2.14) is not valid if $\nu \ll f$, since in this case the electron makes many oscillations before it hits a gas molecule, making the concept of drift velocity inapplicable.

2.3.3 Frequent Electron-Molecular Collisions ($\nu \gg f$)

If ν is neglected as compared to ω in Equation (2.7) we get

$$v_{\text{drift}} = \frac{eE_0}{m\nu} \sin \omega t \quad (2.16)$$

It is seen that in this case the motion of electrons is always in phase with the field. Therefore the motion of electrons is determined solely by their mobility where the mobility is given by $e/m\nu$.

Neglecting ω as compared to ν in Equation (2.15) gives

$$E_{\text{eff}}^2 = E_{\text{rms}}^2 \quad (2.17)$$

2.4 Selection of Optimal r. f. Frequency and Pressure (Collision Frequency)

Ionization of the gas is necessary for photon production. For the condition $\nu \ll f$, the electrons oscillate out of phase with the field, and the scarcity of collisions makes the energy transfer to the electrons an inefficient process necessitating higher breakdown fields.

For the conditions $\nu \gg f$, the efficiency of energy transfer is high, but the number of collisions is also high to the extent that a substantial amount of energy is utilized in elastic collisions, therefore, requiring increased breakdown fields. From this reasoning it appears that for the minimum value of breakdown field the optimum condition is $f_1 \lesssim \nu \lesssim f_2$. Also, as indicated in Section 2.2 an optimal pressure exists between the extremes of high and low pressure for the maximum transfer of resonance radiation through the ionized media to the surface. The above considerations lead to the conclusion

that the condition $f_1 \lesssim \nu \lesssim f_2$ should be satisfied while staying from the extremes in pressure for efficient photon production. In later sections numerical values for ν will be obtained.

CHAPTER III

DESIGN OF THE ULTRAVIOLET SOURCE

3.1 Background

The ultraviolet source is designed with the assumption that the gases to be used are hydrogen and air, since much of the experimental data which is vital for the design exists for these gases only. The optimum design of the ultraviolet source for hydrogen and air is believed to be nearly optimum for krypton as well; experimental observations verify this. The UV sources will be designed with top priority given for achieving lowest possible breakdown fields. The condition that $f_1 \lesssim \nu \lesssim f_2$ for a given ν (pressure) leads to a wide range in the selection of f . From Figure 3.1 the collision frequency of hydrogen can be approximated by 6×10^9 p Hz. If the pressure is arbitrarily selected to be .15 Torr such that it is away from the extremes, then $\nu = 900$ MHz. Quite different design problems arise for $f_1 = \nu/10 < f \lesssim \nu$ than for $\nu \lesssim f < 10\nu = f_2$. Consequently the design of two ultraviolet sources will be considered, $90 \text{ MHz} < f < 900 \text{ MHz}$ (lower frequency) and $900 \text{ MHz} < f < 9000 \text{ MHz}$ (higher frequency).

3.2 Design of the Lower Frequency Source

A coaxial cylinder was selected to contain the gas. One end of the cylinder was fitted with a lithium fluoride window, which has a lower limit of transmission of 1040 \AA . The choice of window depends upon the desired output spectra and the possible radiation frequencies which are to be filtered out. The other end of the cylinder was

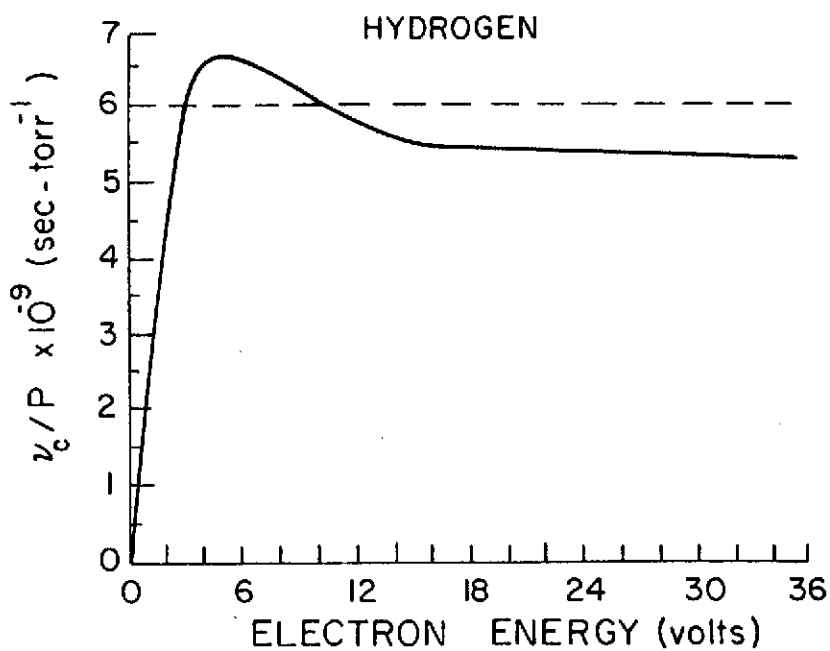
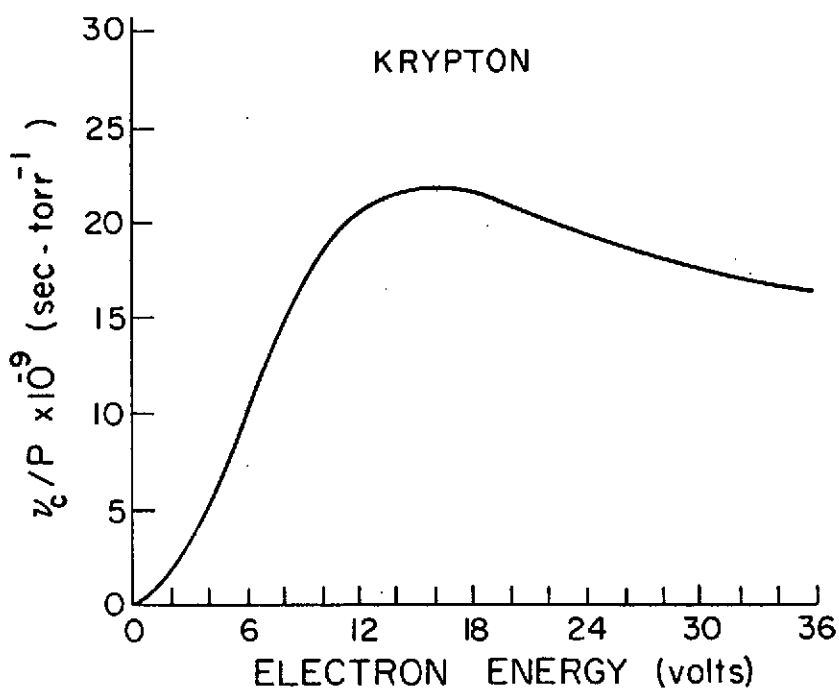


Figure 3.1 Ratio of Electron Collision Frequency to Pressure for Hydrogen and Krypton as a Function of Frequency

closed by a metal plate containing a teflon insulated center conductor. Breakdown of the gas in the cylinder can be achieved by the application of a voltage of sufficient magnitude across the inner and outer conductors to produce the required ionizing E field. This can be done by using the cylinder as the capacitor of a series resonant circuit (at resonance large circulating currents develop a high E field within the capacitor) serving as both the frequency selective and the feedback portions of a transistor power oscillator as illustrated in Figure 3.2. In order to optimize the radii of the inner and outer conductors which will give the minimum value of E field required for breakdown, we will discuss briefly the relation of the resonator geometry to the ionization process.

We are interested in calculating the breakdown field for the condition that $90 \text{ MHz} < f < 900 \text{ MHz}$ and the pressure is about .15 Torr. Here only two significant processes occur, ionization due to electron-molecule collisions, and diffusion of electrons and ions to the resonator walls (from Equation (2.9) the amplitude of oscillation of electrons for the above conditions is much smaller than the distance between the inner and outer conductors of resonators to be used, so that electrons are not swept to the walls by the field). Ion-molecule collisions are neglected due to the large mass of ions. In certain gases electrons can be effectively removed by attachment to gas molecules also; loss by recombination is usually negligible, except when the concentration of charges are large. Breakdown will take place if, on the average, a new electron is produced by ionization for each one that diffuses out of the container. Therefore, if the

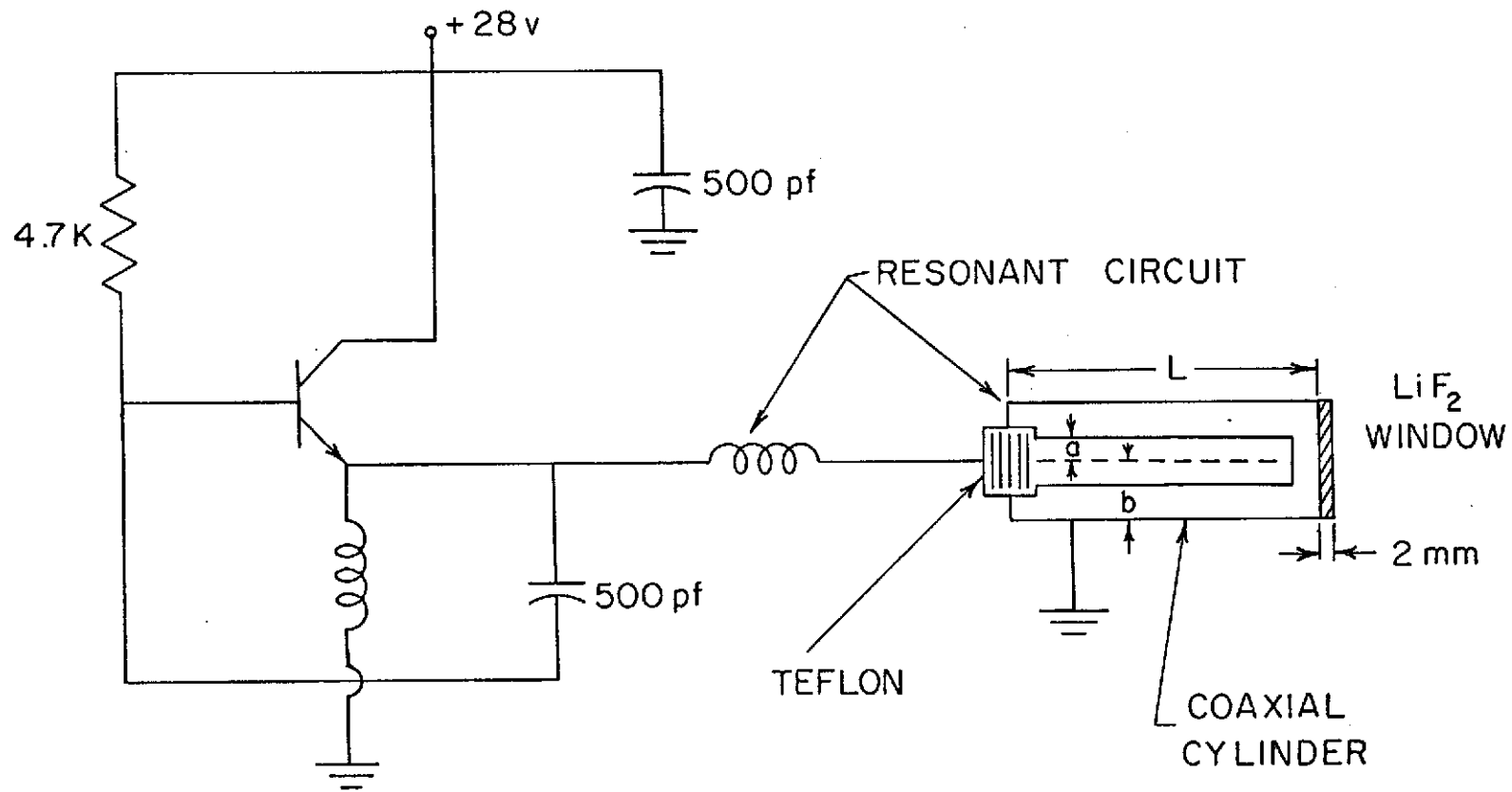


Figure 3.2 Schematic for Lower Frequency Source

number of collisions an average electron must make before gaining enough energy to reach ionization potential is equated to the number of collisions an electron makes in diffusing out of the container, we have a breakdown criterion.

The energy gained between collisions by the electron in the electric field is found as the change in the average value of the square of the drift velocity

$$\langle \Delta v^2 \rangle = \left\langle \left(\frac{E_e e}{m} \right)^2 (\Delta t)^2 \right\rangle \quad (3.1)$$

where E_e is the effective field, Δt is the time between collisions. The average value of $(\Delta t)^2$ is $2/\nu^2$, and the change in energy between collisions, expressed in units of voltage, is given $\langle \frac{m}{2e} (\Delta v^2) \rangle$; we therefore have the energy change between collisions

$$\Delta u = \frac{E_e^2 e}{m\nu} \quad (3.2)$$

Dividing this into the ionization energy we obtain the average number of collisions required for an electron to reach ionization energy

$$N_{ion} = \text{Ionization energy } (u_i) / \Delta u \quad (3.3)$$

To find the average number of collisions required for an electron to diffuse out of the container we first find the root mean square of the distance traveled in N collisions which is given (Kennard, 1938) to be

$$\langle \Lambda^2 \rangle = 2 \ell^2 N/3 \quad (3.4)$$

If this distance, Λ , is called the characteristic diffusion length Λ (see Appendix A), the number N is given by

$$N_{\text{diff}} = 3/2 (\Lambda^2/\ell^2) \quad (3.5)$$

where ℓ is the mean free path $= \lambda_e$. Equating the number of collisions required for an average electron to reach ionization energy to the number of collisions required for an average electron to diffuse out of the resonator $N_{\text{ion}} = N_{\text{diff}}$, we obtain $m u_i v^2 / E_e^2 = 3/2 \Lambda^2 / \ell^2$ which leads to

$$E_e^2 = 2/3 \frac{\ell^2 m u_i v^2}{\Lambda^2_e} \quad \text{or} \quad E_{\text{applied}}^2 = \left(\frac{v^2 + \omega^2}{v^2} \right) \left(\frac{2 \ell^2 m u_i v^2}{3 \Lambda^2_e} \right) \quad (3.6)$$

Exact calculations of minimum breakdown field for $f_1 \lesssim \nu \lesssim f_2$ are difficult if not impossible. However, to obtain a rough estimate asymptotic approximations will be used, i. e., the easily obtained expressions for E field when $\nu \gg f$ and for E field when $\nu \ll f$ will be equated. For $\nu \ll \omega$

$$E^2 = \frac{2 \ell m u_i \omega^2}{3 \Lambda^2_e} \quad (3.7)$$

The ionization energy for hydrogen is 15.4 volts. The value of $\ell = \lambda_e$ is chosen to correspond to an electron energy near the ionization energy and can be found from the collision frequency given by Figure 3.1. This choice of ℓ is necessary since at low pressures the average electron energies are much higher than they are at higher

pressures; at high pressure elastic collision losses prevent many electrons from reaching high energies. Knowing l , u , and m/e for hydrogen we can write Equation (3.7) as

$$E \approx \frac{550}{p\lambda\Lambda} \quad (3.8)$$

Figure 3.3 indicates that at high pressures, i. e., $\nu \gg f$, the required field for ionization is quite independent of frequency and can be expressed as

$$E \approx 10 p \quad (3.9)$$

A simultaneous solution of Equations (3.8) and (3.9) is expressed as

$$\frac{1}{\Lambda^2} = \left(\frac{p^2 \lambda}{55} \right) \quad (3.10)$$

Substituting the value of $1/\Lambda^2$ for a coaxial geometry from Appendix A we have

$$\left(\frac{.331}{a} \right) + \left(\frac{\pi}{2L} \right) = p^4 (\lambda/55)^2 \quad (3.11)$$

where a is the inner conductor radius and L is the length of the coaxial cylinder. Equation (3.10) is valid for the ratio $h = b/a = 10$ where b is the outer conductor radius. A family of curves for a vs. p for different values of $\lambda = c/f$ for $h = 10$ and $L = 2.5$ cm are drawn in Figure 3.4. Different sets of values for h and L will give additional family of curves. Specifying h and L arbitrarily, optimum breakdown field can be obtained for any desired pressure by selecting the appropriate value of a . The details of this procedure are found in Appendix A.

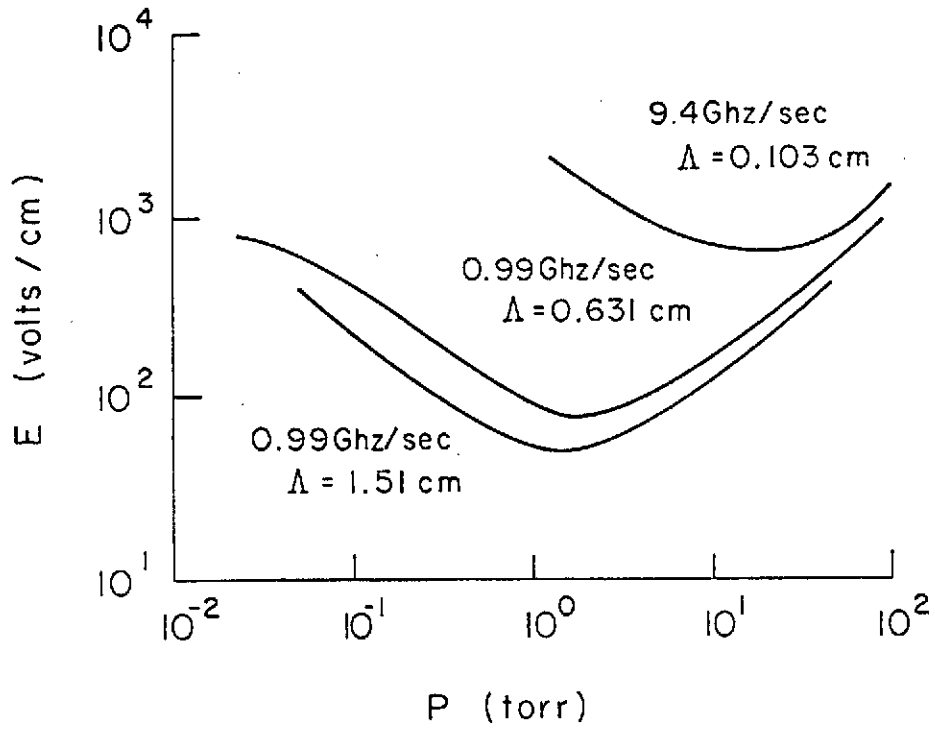


Figure 3.3 Experimental Breakdown Data in Hydrogen

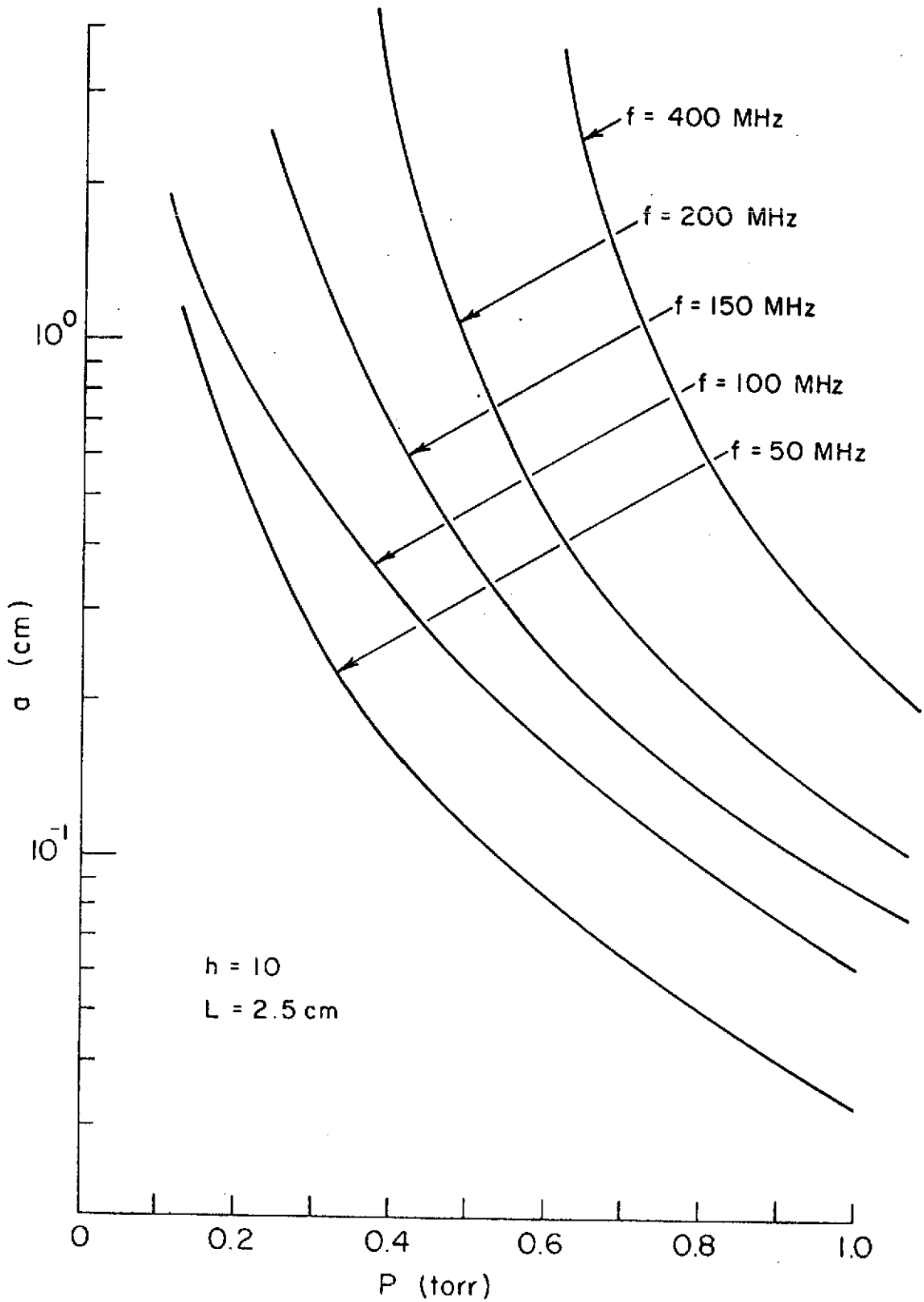


Figure 3.4 Family of Curves for a vs. p for Minimum Breakdown Field

A low frequency source, with parameters ($a = .2$ cm, $f = 100$ mc, $p = .2$ Torr and $L = 2.5$ cm) chosen in the light of the above discussion and the convenience with which these parameters could be realized in practice, was built. The results obtained from this source are discussed in Chapter IV.

3.3 Design of the Higher Frequency Source ($900 \text{ MHz} \lesssim \nu \lesssim$ 9000 MHz)

It is incorrect to apply lumped element concepts to the design of the higher frequency gas container as was done for the lower frequency case. Instead, transmission line concepts must be employed; in particular, a coaxial quarter wave resonator was selected to contain the gas with a lithium fluoride window placed at the high impedance end. In this container the electric field is not uniform, regardless of the method used in coupling energy into it. The non-uniformity of the E-field necessitates the use of a different procedure than the one used in the design of the lower frequency case and is explained in Appendix B. A plot of the breakdown voltage as a function of b/a for different values of pa ($p = 1$ mm) for a given $p\lambda$ ($\lambda = 20$ cm) is shown in Figure 3.5 and is obtained from Appendix B.

The choice of $p = 1$ mm is high as compared to $p = .15$ mm used in the low frequency case, which was indicated as a possible optimum for resonance radiation transport out of the ionized media. But in the high frequency case transport of radiation out of the ionized media is not nearly as important because ionization takes place only at the high voltage end of the cavity which is directly behind the window. Hence, p was selected to be 1 mm because it facilitated

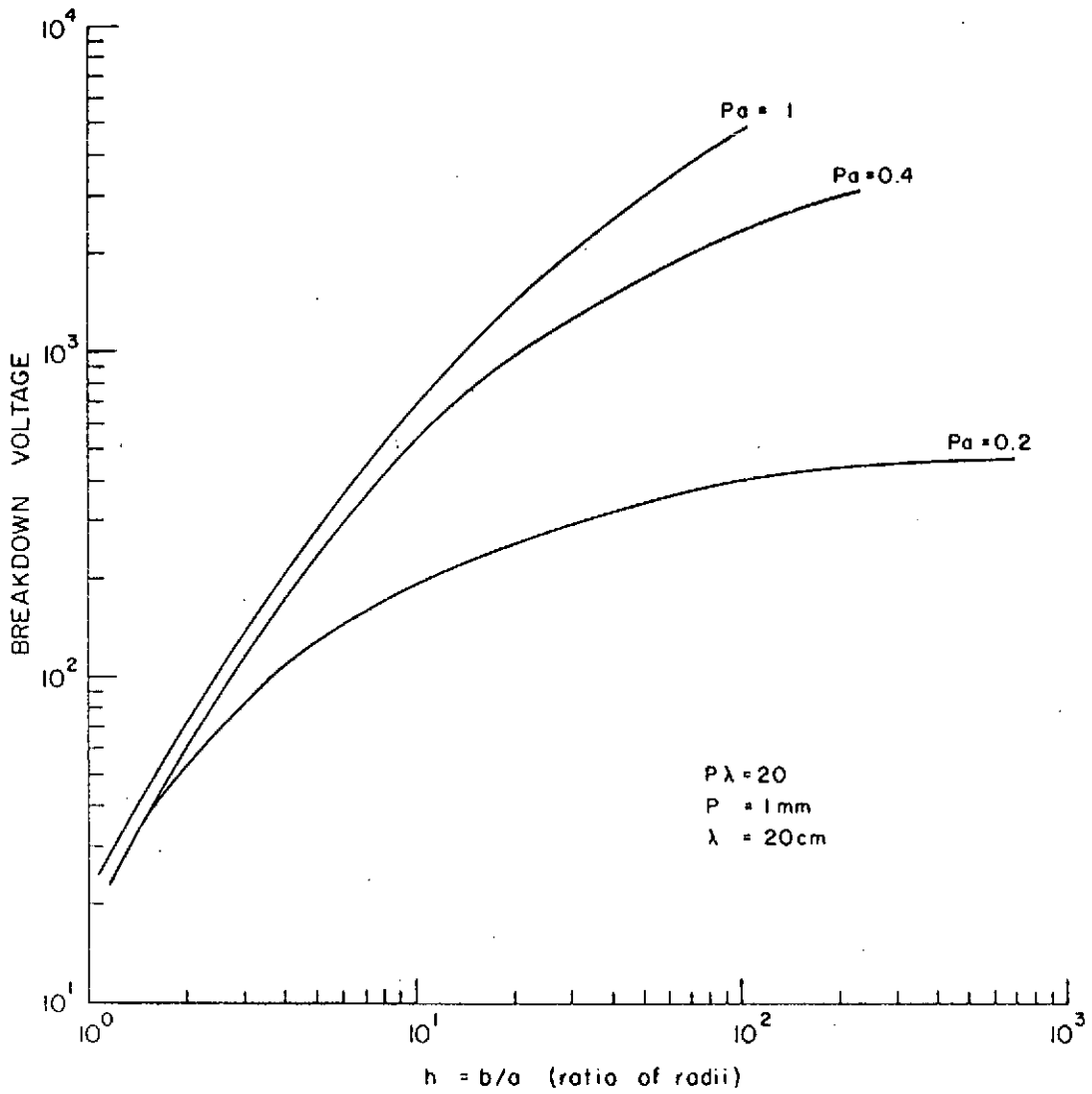


Figure 3.5 High Frequency Breakdown Voltage Between Coaxial Cylinders as a Function of b/a and pa

the use of data given by Figures B. 1, B. 2 and B. 3, and as indicated in the lower frequency case this pressure change should not alter ease of ionization very greatly. For $\lambda = 20$ cm and $p = 1$ mm the choice of a convenient value of $h = 8$ gives the value of $a = .2$ cm for minimum value of breakdown voltage. With these values for a and h a resonator was built with $L = \lambda/4 = 5$ cm.

Different methods of coupling energy into the gas container were used. The quarter wave anode-grid cavity of a 1680 MHz R. C. A. 5794 telemetry tube was combined with the gas container to form a half wave resonator as shown in Figure 3. 6. The frequency of oscillation is nearly the same as for the original tube. The feedback is primarily internal through the anode-cathode capacitance. The voltage at the window end of the container is higher than that at the grid-anode cross section of the tube since Z_{02} is higher than Z_{01} . Consequently the discharge takes place just behind the window. The results are discussed in Chapter IV.

A voltage step-up was also achieved for cases in which the cross section of the gas container did not vary, i. e., the impedance of the coaxial line used in the anode-grid cavity was invariant with position. The step-up voltage at window end from that at the grid-anode gap was achieved by physically moving the grid-anode gap closer to the junction of the cavities while keeping the $\lambda/4$ electrical length of the grid-anode cavity by adding capacitance at the grid-anode gap. In this method the gas container was not designed for optimum breakdown since the goal was to keep the radii of the container the same as the original grid-anode cavity of the tube for convenience.

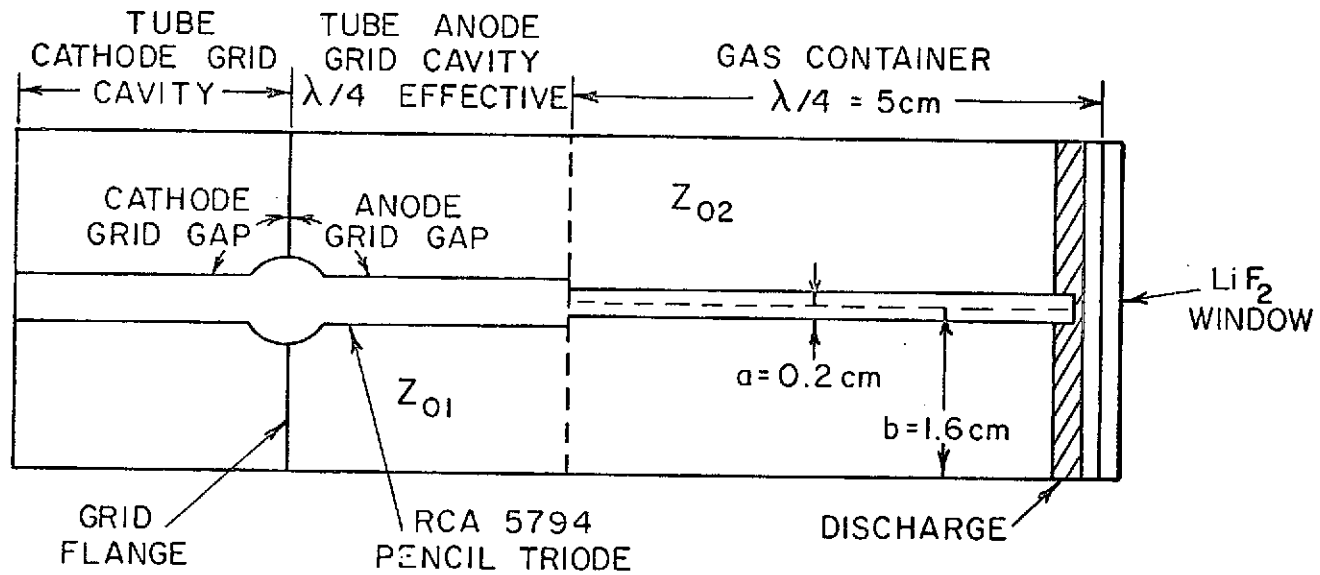


Figure 3.6 Schematic of the "Stepped" Cavity Version of the Higher Frequency Source

This can be used to further enhance the "stepped" cavity previously described. Although the system oscillated as predicted and with great strength the discharge was not obtained, thereby underscoring the need for designing the container for minimum breakdown field.

CHAPTER IV

RESULTS AND INTERPRETATIONS

The breakdown optimization techniques of Chapter III were applied to the design of a lower frequency ($f_1 \lesssim \nu$) and a higher frequency ($\nu \lesssim f_2$) UV source. These sources were constructed and test results are compared with each other and with the predictions of Chapter III. Special note is made of critical factors in optimization of photon output.

4.1 Optimum Photon Output as a Function of Gas, Pressure and Frequency, Etc.

Maximum photon output for the lower frequency source (l. f. s.) was 5×10^{14} photons/sec with krypton for a pressure of .2 Torr. For the same pressure the photon output dropped to 5×10^{13} photon/sec with hydrogen. The maximum photon output for the higher frequency source (h. f. s.) was about 2×10^{13} photons/sec and 1×10^{13} photons/sec with krypton and hydrogen respectively for a pressure of 1 Torr. The greater increase in photon output in the lower frequency source as compared with the higher frequency source when krypton is used instead of hydrogen may be attributed to the larger volume of ionization in the lower frequency source.

Maximum photon output was obtained at a pressure of .2 Torr and 1 Torr for the l. f. s. and h. f. s., respectively. The photon maximum at .2 Torr in the l. f. s. suggests an optimum compromise between resonance radiation transport phenomena and the number of atoms available to be put into the excited states once ionization has

taken place. The maximum photon output in the h. f. s. occurred at a higher pressure than was anticipated. Here resonance radiation transport phenomena is less significant because the ionization takes place in a small volume just behind the window, and it is more important to have a higher number of atoms available to be put into the excited states for maximum photon output.

In the l. f. s. as the applied frequency was varied between 100 and 300 MHz no noticeable change in photon output was experienced. Frequencies above 500 MHz were not used because of the difficulty of using lumped elements in this range. In h. f. s. the frequency used was about 1700 MHz.

Cleaning of the lithium fluoride window with benzene increased the photon output an order of magnitude. Unfortunately this was observed when working on the l. f. s. and work for the h. f. s. was completed. Thus the photon output for the h. f. s. could have been higher had this effect been observed earlier.

4.2 Saturation of Photon Output with Increased Input Power

It was observed that the photon output was not a linear function of input power in both the l. f. s. and h. f. s. ; it leveled off at certain amount of r. f. input power. A possible explanation for this phenomena can be given if the amplitude of electron oscillation is taken into consideration. From Equation (2.9) the amplitude is $eE_0 / m\omega \sqrt{v^2 + \omega^2}$; for a given pressure and frequency the amplitude is proportional to E_0 , which is proportional to input power. Thus increasing the input power increases the amplitude of electron oscillations which when comparable to the distance between inner and outer conductors causes

an additional loss of electrons from the ionized media to the walls of the resonator. A limitation (and even a possible reduction) in the intensity of ionization and, hence, in photon production results. In order to increase the photon output by increasing input power beyond this saturation level the distance between the inner and outer conductors should be increased and appropriate values of 'a' and 'h' can be selected from Figure 3.5. This will alter the breakdown conditions from minimum required E, but an optimization of required E can still be achieved for constraint of photon output by using methods of Chapter III.

4.3 Effect of Superimposing DC Field on AC Field

A DC field was superimposed on the applied AC field in the low frequency case. It was observed that the DC field changed the pattern of the discharge inside the resonator; depending upon the polarity of the applied DC field the discharge could be concentrated near the center conductor or the outer conductor. It was not possible to initiate ionization with DC field superimposed on the AC field, and there was a very slight increase in photon output if the DC field was superimposed after ionization took place.

These effects can possibly be explained by realizing that the ionization depends not only upon the magnitude of the field, but also upon its frequency, the collision frequency, and the characteristic length of the container. Ionization can occur during two portions of an r.f. cycle. If a DC field of comparable strength to the r.f. field is superimposed, the ionization is reduced to one period of the r.f. cycle, while the time of deionization (loss of electrons by diffusion

to the walls of the resonator) is increased. The increase in ionization by increased electron velocities is not enough to offset the increase in deionization thereby requiring a higher ionization AC field and only a slight increase of ionization intensity once ionization has taken place. However, once ionization has been initiated it appears that sufficient excess electrons exist such that this increased deionization time is insufficient to overcome the increase in ionization which occurs when the DC and r. f. fields add.

4.4 Ionization Field

The ionization of the gas was achieved with ease for the pressure range .1 Torr to 1 Torr in both l. f. s. and stepped inner conductor version of h. f. s. which suggests that the applied E field was well above the minimum required for ionization. This provides a degree of confidence in the optimizing methods of Chapter III.

CHAPTER V

CONCLUSIONS

Ultraviolet sources for the lower and higher frequencies have been designed and fabricated with the data available for hydrogen and air. It was found that these designs gave similar results for krypton as well with only slight modifications in the container dimensions, though this does not imply that these are optimum designs for krypton. To determine the optimum design for krypton or an other desired gas, experimental data such as that available for hydrogen and air is required; the remainder of the procedure is as indicated in Sections 3.2 and 3.3.

The photon output of the sources decreased gradually as a function of time. The possible reasons for this include the deterioration of the transmission properties of lithium fluoride window and the increase in pressure of the gas in the container. It is suggested that magnesium fluoride window be used instead of lithium fluoride; these have been used by Young (1967) with improved performance in his design of the UV source.

The lower frequency source is more efficient than the higher frequency source. It is very likely that the photon output of the lower frequency source can be further increased if additional time is spent to empirically obtain an optimum compromise between the ease of breakdown of the krypton gas and photon output, though variations of container dimensions, and gas pressure.

APPENDIX A

Calculation of the breakdown field for the condition that $f_1 < v < f_2$ requires only including two processes as significant, ionization due to electrons colliding with gas molecules, and diffusion of electrons to the walls of the resonator. With the rate of diffusion specified by a diffusion coefficient D , we define a diffusion potential as the product of the diffusion coefficient D and the electron concentration n ; the current flowing in the gas due to diffusion is given by

$$\bar{J} = -\nabla(Dn)$$

where \bar{J} is the current density. The continuity equation for electrons is

$$\frac{\partial n}{\partial t} + \nabla \bar{J} - ni = 0 \quad (\text{A. 1})$$

where i is the ionization rate per electron. Assuming that the diffusion coefficient is independent of spatial variations, we can write Equation (A. 1) as

$$\frac{1}{n} \frac{\partial n}{\partial t} - \sqrt{i} = \frac{D}{n} \nabla^2 n \quad (\text{A. 2})$$

If the ionization rate is independent of spatial variations, both sides of equation can be set to a constant, k , so that

$$\nabla^2 n = -\frac{kn}{D} = -k_c^2 n \quad \text{and} \quad (\text{A. 3})$$

$$\frac{\partial n}{\partial t} = (\sqrt{i} - k)n$$

For gas enclosed in a coaxial cylinder, as shown in Figure A. 1,
Equation (A. 3) becomes

$$\nabla^2 n + k_c^2 n = \frac{1}{r} \frac{\partial}{\partial r} \left(r \frac{\partial n}{\partial r} \right) + \frac{1}{r^2} \frac{\partial^2 n}{\partial \phi^2} + \frac{\partial^2 n}{\partial z^2} + k_c^2 n = 0$$

A product solution of the form

$$n = R(r) \Phi(\phi) Z(z)$$

is assumed and the method of the separation of variables yields the following set of equations:

$$d^2 \Phi / d\phi^2 + p^2 \Phi = 0 \quad (\text{A. 4})$$

$$\frac{d^2 Z}{dz^2} + q^2 Z = 0 \quad (\text{A. 5})$$

$$\frac{d^2 R}{dr^2} + \frac{1}{r} \frac{dR}{dr} + (-q^2 + k_c^2 - p^2/r^2) R = 0 \quad (\text{A. 6})$$

Equation (A. 3) has a solution

$$\Phi = A \sin p\phi + B \cos p\phi \quad (\text{A. 7})$$

while the solution of Equation (A. 5) is

$$Z = C \sin qz + D \cos qz \quad (\text{A. 8})$$

Equation (A. 6) is almost a Bessel equation and would be exactly one if $(k_c^2 + q^2)$ were replaced unity. This can be done by letting $R(r) = R_1(\sqrt{-q^2 + k_c^2} r)$ and defining $\sqrt{-q^2 + k_c^2} r = r_1$; then Equation (A. 6) becomes $d^2 R_1 / dr_1^2 + 1/r_1 dR_1 / dr_1 + (1 - p^2/r_1^2) R_1 = 0$. This is

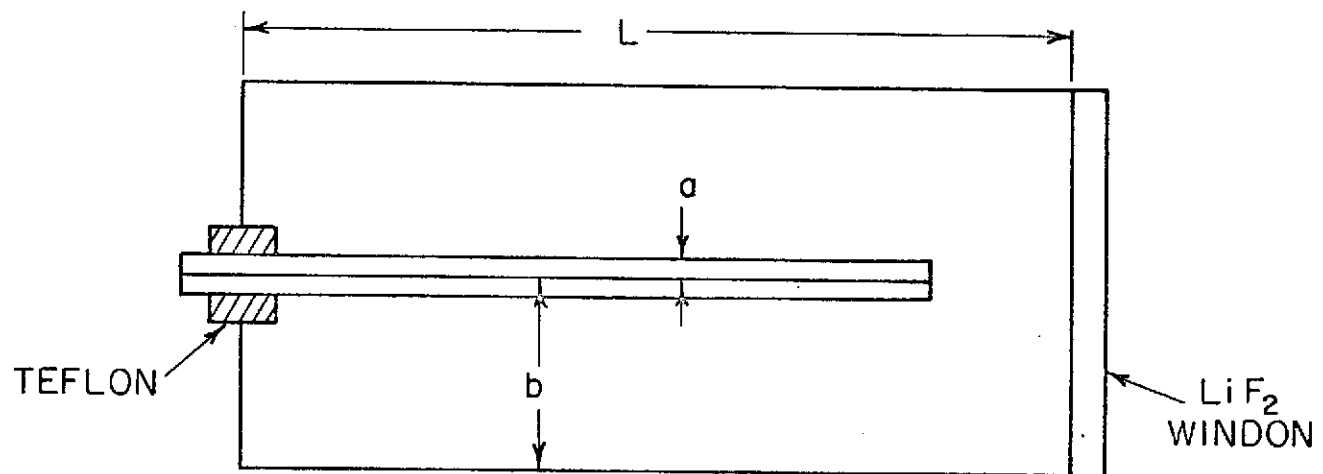


Figure A. 1 Gas Container for the Lower Frequency Source

Bessels' equation of order p with r_1 , as the variable which has a general solution

$$R(r_1) = R(r) = E J_p(r_1) + F N_p(r_1)$$

where J_p and N_p are Bessel functions of the first and second kind, respectively. Thus the general solution for n is

$$n = (A \sin p \phi + B \cos p \phi) (C \sin q z + D \cos q z) \left[B J_p(r_1) + F N_p(r_1) \right]$$

It remains now to evaluate the constants. 'A' may be set equal to a zero arbitrarily, since this merely amounts to rotation of the system to a point where the harmonic variation in ϕ appears as a simple cosine function rather than a combination of sine and cosine terms. Next, the solution must be periodic in ϕ with a period of 2π since n is a single-valued function of r and ϕ . Thus p must be restricted to integral values (zeros included). The solution reduces to

$$n = B \cos p \phi (C \sin q z + D \cos q z) \left[E J_p(r_1) + F N_p(r_1) \right]$$

where p can take on only integral values. Applying the boundary condition that $n = 0$ at $z = 0$ and $dn/dz = 0$ at $z = L$, which is true for all r and ϕ , since no electrons are moving past the window or exist at the walls of the resonator. Thus $D = 0$ and $C q \cos q L = 0$ or $q = \gamma \pi / 2L$, where $\gamma = 1, 3, \dots$. From practice, the electron distribution is expected to have no variation in ϕ which corresponds to $p = 0$

and only the lowest order variation in z , i. e., $y = 1$. Applying the boundary condition that $n = 0$ at $r = a$ and $r = b$, which is true for all values of z and ϕ , with $p = 0$ and $y = 1$ gives

$$\frac{J_0 \left[\sqrt{k_c^2 - (\pi/2L)^2} a \right]}{N_0 \left[\sqrt{k_c^2 - (\pi/2L)^2} a \right]} = -F/E$$

$$\frac{J_0 \left[\sqrt{k_c^2 - (\pi/2L)^2} b \right]}{N_0 \left[\sqrt{k_c^2 - (\pi/2L)^2} b \right]} = -F/E$$

or

$$\frac{J_0 \left[\sqrt{k_c^2 - (\pi/2L)^2} a \right]}{N_0 \left[\sqrt{k_c^2 - (\pi/2L)^2} a \right]} = \frac{J_0 \left[\sqrt{k_c^2 - (\pi/2L)^2} b \right]}{N_0 \left[\sqrt{k_c^2 - (\pi/2L)^2} b \right]} \quad (\text{A. 9})$$

Let $u = \sqrt{k_c^2 - (\pi/2L)^2} a$ and define $h = b/a$ so that Equation (A. 9) becomes

$$\frac{J_0(u)}{N_0(u)} = \frac{J_0(uh)}{N_0(uh)} \quad (\text{A. 10})$$

Solving for the first root of Equation (A. 10), since lowest order solution is required, we obtain (Watson, 1952)

$$(h - 1) u' = 2.983 \text{ or } u' = .331$$

therefore

$$\sqrt{k_c^2 - (\pi/2L)^2} a = .331 \text{ or } k_c^2 = (.331/a)^2 + (\pi/2L)^2 .$$

Since $k_c^2 = k/D$ has the dimensions of reciprocal of distance squared, it is written as $k/D = 1/\Lambda^2$, which defines Λ as the characteristic diffusion length.

APPENDIX B

The continuing equation for electrons is as before (See Appendix A) $\partial n / \partial t + \bar{\nabla} \bar{J} - n\nu = 0$. In the higher frequency case, $\bar{J} = -\bar{\nabla}(Dn) = -D \bar{\nabla}n - n\bar{\nabla}D$; $-D\bar{\nabla}n$ is the diffusion current density and $-n\bar{\nabla}D$ is the current density due to the kinetic energy gradient, which is present due to the non-uniformity of the E-field in the resonator. The continuity equation now becomes

$$\frac{1}{n} \frac{\partial n}{\partial t} - \nu = D/n \nabla^2 n + \nabla^2 D \quad (\text{B. 1})$$

From Equation (B. 1) it is clear that the procedure used to obtain the breakdown field by calculating Λ in the lower frequency case is not applicable here because of the additional term $\nabla^2 D$. The breakdown condition from Equation (A. 1) is

$$\nu n + \nabla^2 (Dn) = 0 \quad (\text{B. 2})$$

Equation (B. 2) can be rewritten as $\nabla^2 (Dn) + \nu DnE^2 / DE^2 = 0$, or,

$$\nabla^2 (Dn) + \zeta DnE^2 = 0 \quad (\text{B. 3})$$

where $\zeta = \nu / DE^2$, and is defined as the high frequency ionization coefficient (Herlin and Brown, 1948). The solution of Equation (B. 3) for particular geometries, with the use of ζ derived from uniform field measurements, leads to calculated breakdown fields in good agreement with those found by experiment (Herlin and Brown, 1948), and will be discussed below.

For a quarter wave coaxial resonator the electric field is given by

$$E = (V/r \ell n b/a) \sin \pi z/2L \quad (B. 4)$$

where V is the voltage at the center conductor, a and b are the inner and outer conductor radii, L is the length of the cavity, r and z are the radial and axial space coordinates. Substitution of this value of E in Equation (B. 3) leads to a non-separable equation. If it is assumed that a is much smaller than L, the electric field in the region near the center conductor where ionization will occur due to the large value of E does not vary much with distance along the conductor; in that case

$$E = V/r \ell n b/a \quad (B. 5)$$

The plot of ζ for air vs. E/p with $p\lambda$ as a parameter, obtained by Herlin and Brown (1948) for uniform fields between parallel plates, is shown in Figure B. 1. From Figure B. 1 and Equation (B. 5) ζE^2 can be computed as a function of position. With this approximation Equation (B. 4) is a second-order linear differential equation in r only. To solve Equation (B. 3) numerical integration must be used since ζ is given from numerical data. Herlin and Brown (1948) have shown that ζ can be approximated by $\zeta_a (E/E_a)^{\beta-2}$ with results within one percent of agreement with that obtained from numerical integration. ζ_a and E_a are the values for ζ and E at $r = a$. $(\beta-2)$ is the slope of curve in Figure B. 1 on a logarithmic plot for the value of E/p at $r = a$ on the appropriate $p\lambda$

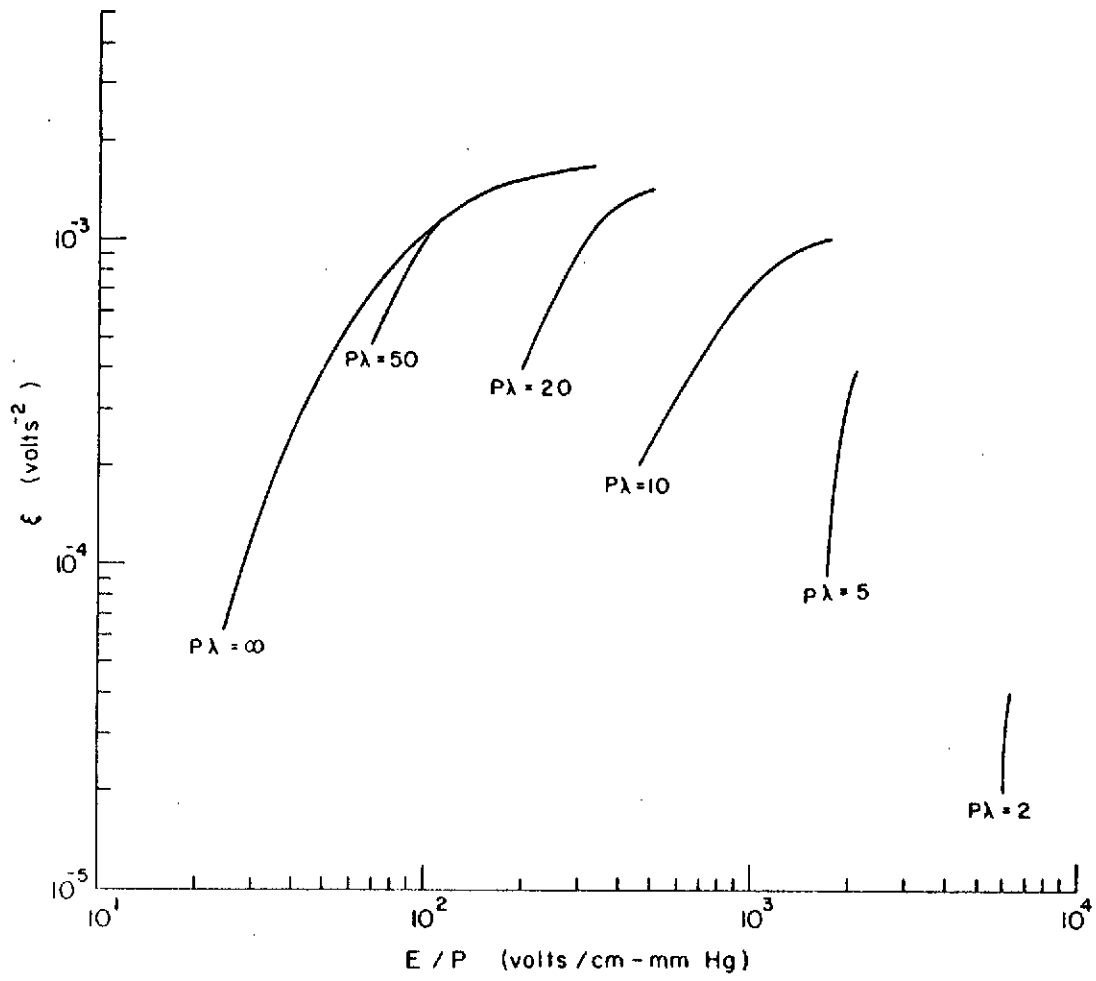


Figure B. 1 High Frequency Ionization Coefficients as a Function of E/p and $p\lambda$

curve, and is shown in Figure B. 2. In general the above approximations are accurate near the center conductor only, but if b/a is small they are accurate throughout the entire cavity. For large values of b/a this approximation can still be used with slight inaccuracy because the ionization is most pronounced near the center conductor. Using the approximate value of ξ and combining Equations (B. 3) and (B. 5) we get

$$\frac{d^2 D_n}{dr^2} + \frac{1}{r} \frac{dD_n}{dr} + k^2 (a/r)^\beta D_n = 0 \quad (B. 6)$$

where $k^2 = \xi_a E_a^2$ and whose solution is

$$D_n = Z_0 \left[\frac{2}{\beta-2} k a (a/r)^{(\beta-2)/2} \right] \quad (B. 7)$$

where Z_0 is the zero order solution of Bessel's equation. Applying the boundary condition that $D_n = 0$ at $r = a$ and $r = b$ we get

$$J_0(m) N_0 \left[(b/a)^{(\beta-2)m/2} \right] - J_0 \left[(b/a)^{(\beta-2)m/2} \right] N_0(m) = 0 \quad (B. 8)$$

where $m = 2/\beta - 2 \quad ka (a/b)^{2/(\beta-2)}$. Roots of this equation are tabulated (Watson, 1952), giving m as a function of $(b/a)^{2/(\beta-2)}$. Multiplying m by $(b/a)^{2/(\beta-2)}$ we get the curve of Figure B. 3, which gives $[2/(\beta-2)] ka$ as a function of $(b/a)^{2/(\beta-2)}$.

To find the breakdown voltage, V as a function of b/a , the following procedure is used:

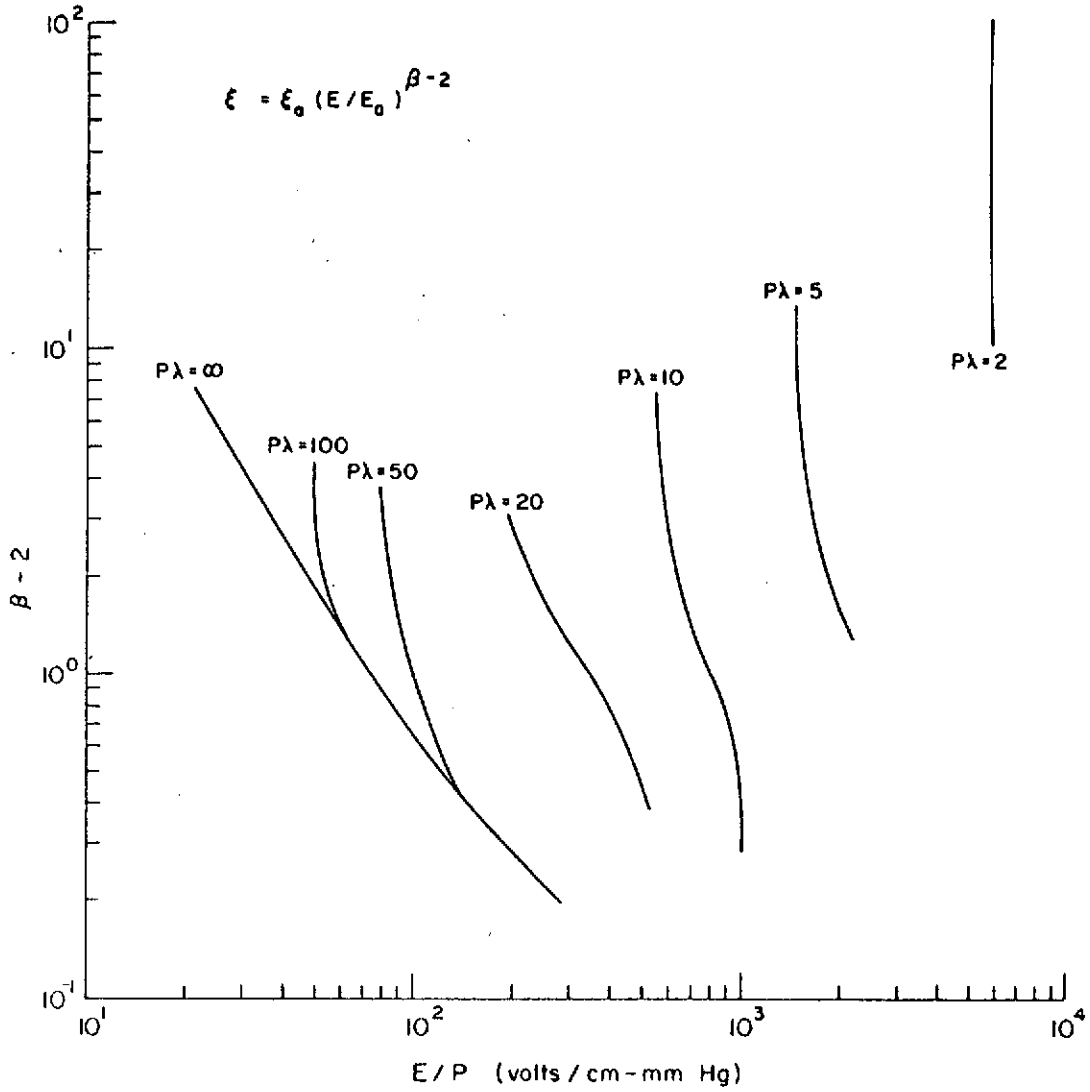


Figure B. 2 Slope of ξ versus E/p Curve on Log Plot from Figure B. 1

- (a) Pressure (p) and frequency (λ) are selected in Chapter II.
- (b) The radius of the inner conductor (a) is chosen for convenience.
- (c) From Figures B. 1 and B. 2 k^2/E_a^2 and $(\beta - 2)$ are obtained for any desired value of E_a/p . Then $2k_a/(\beta - 2)$ is computed from these, which gives $(b/a)^{2/(\beta - 2)}$ from Figure B. 3. From this latter b/a and V are calculated using Equation (B. 5).

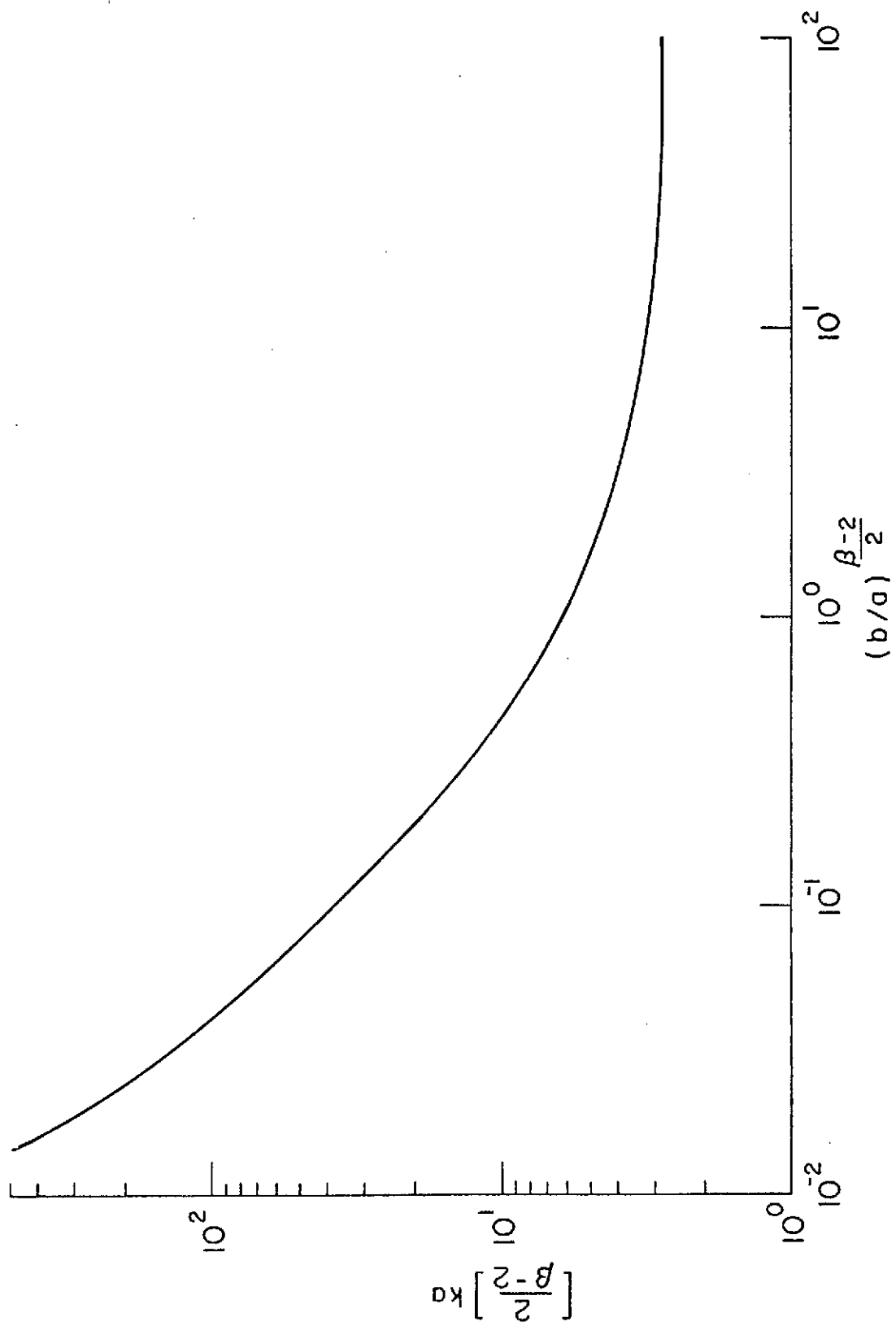


Figure B.3 Solution of Equation (B.8)

REFERENCES

- Bekefi, G., J. Hershfield and S. C. Brown, Incoherent microwave radiation from plasma, Phys. Rev., 116, 1051, 1959.
- Brown, S. C., Introduction to electrical discharge in gases, John Wiley and Sons, 1966.
- Francis, G., Ionization phenomena in gases, Academic Press, London, 1960, p. 51.
- Gee, E. L., A subsonic D-region probe experiment using an ultraviolet source to produce ions and free electrons, Scientific Report No. 286, Ionosphere Research Laboratory, The Pennsylvania State University, 1965.
- Herlin, M. A. and S. C. Brown, Phys. Rev., 74, 291, 910, 1650, 1948.
- Holstein, T., Imprisonment of resonance radiation in gases, Phys. Rev., 72, 1212, 1947.
- Kennard, E. H., Kinetic theory of gases, McGraw-Hill, 1938, p. 273.
- Lorentz, H. A., Theory of electrons, Leipzig: Teubner, 1916.
- MacDonald, A. D. and S. C. Brown, Canad. J. Phys., 28, 168, 1950.
- MacDonald, A. D., Microwave breakdown in gases, John Wiley and Sons, 1966.
- Okabe, H., Intense resonance line sources for photochemical work in the vacuum ultraviolet region, J. Optical Society of America, 54, 478, 1964.
- Pontano, B. A., Rocket measurements of nitric oxide in the lower D-region of the ionosphere, a doctoral thesis in Electrical Engineering, Ionosphere Research Laboratory, The Pennsylvania State University, 1970.
- Schleg, E. W. and F. J. Comes, Intense light sources for the vacuum ultraviolet, J. Optical Society of America, 50, 866, 1938.
- Townsend, J. S. and E. W. R. Gill, Phil. Mag., 26, 290, 1938.
- Watson, G. N., Theory of Bessel functions, Cambridge University Press, Cambridge, 1952.

Wilkinson, P. G. , New krypton light source for the vacuum ultraviolet, J. Optical Society of America, 45, 1045, 1955.

Young, R. A. , Measurement of nitric oxide in the earth's atmosphere, Final Report, Stanford Research Institute, Project PAU-3895, 1967.